Structure and component dynamics in binary mixtures of poly(2-(dimethylamino)ethyl methacrylate) with water and tetrahydrofuran: A diffraction, calorimetric, and dielectric spectroscopy study

G. Goracci', A. Arbe, A. Alegría, Y. Su, U. Gasser, and J. Colmenero

Citation: J. Chem. Phys. 144, 154903 (2016); doi: 10.1063/1.4946004

View online: http://dx.doi.org/10.1063/1.4946004

View Table of Contents: http://aip.scitation.org/toc/jcp/144/15

Published by the American Institute of Physics







Structure and component dynamics in binary mixtures of poly(2-(dimethylamino)ethyl methacrylate) with water and tetrahydrofuran: A diffraction, calorimetric, and dielectric spectroscopy study

G. Goracci,^{1,a)} A. Arbe,¹ A. Alegría,^{1,2} Y. Su,³ U. Gasser,⁴ and J. Colmenero^{1,2,5} ¹Centro de Física de Materiales (CFM) (CSIC-UPV/EHU)—Materials Physics Center (MPC), Paseo Manuel de Lardizabal 5, 20018 San Sebastián, Spain

(Received 27 January 2016; accepted 31 March 2016; published online 18 April 2016)

We have combined X-ray diffraction, neutron diffraction with polarization analysis, small angle neutron scattering, differential scanning calorimetry, and broad band dielectric spectroscopy to investigate the structure and dynamics of binary mixtures of poly(2-(dimethylamino)ethyl methacrylate) with either water or tetrahydrofuran (THF) at different concentrations. Aqueous mixtures are characterized by a highly heterogeneous structure where water clusters coexist with an underlying nano-segregation of main chains and side groups of the polymeric matrix. THF molecules are homogeneously distributed among the polymeric nano-domains for concentrations of one THF molecule/monomer or lower. A more heterogeneous situation is found for higher THF amounts, but without evidences for solvent clusters. In THF-mixtures, we observe a remarkable reduction of the glass-transition temperature which is enhanced with increasing amount of solvent but seems to reach saturation at high THF concentrations. Adding THF markedly reduces the activation energy of the polymer β -relaxation. The presence of THF molecules seemingly hinders a slow component of this process which is active in the dry state. The aqueous mixtures present a strikingly broad glass-transition feature, revealing a highly heterogeneous behavior in agreement with the structural study. Regarding the solvent dynamics, deep in the glassy state all data can be described by an Arrhenius temperature dependence with a rather similar activation energy. However, the values of the characteristic times are about three orders of magnitude smaller for THF than for water. Water dynamics display a crossover toward increasingly higher apparent activation energies in the region of the onset of the glass transition, supporting its interpretation as a consequence of the freezing of the structural relaxation of the surrounding matrix. The absence of such a crossover (at least in the wide dynamic window here accessed) in THF is attributed to the lack of cooperativity effects in the relaxation of these molecules within the polymeric matrix. Published by AIP Publishing. [http://dx.doi.org/10.1063/1.4946004]

I. INTRODUCTION

Mixtures are ubiquitous in our daily life. Simply by mixing thermodynamically miscible molecules with different properties, materials accomplishing the desired requirements for their end-use can sometimes be tailored. The interval within which the properties can be tuned depends on the difference between those exhibited by the neat components. This applies, for instance, to the dynamical features—of utmost importance to determine, e.g., the mechanical properties of the material. In this sense, considering two starting systems with very different glass-transition temperatures opens, in principle, a wide range of possibilities for the vitrification temperature range of the mixture. This

Water is the solvent in many binary mixtures including plasticized polymers. The immense relevance of water as

 $^{^{}a)} sckgorag@ehu.es\\$



²Departamento de Física de Materiales (UPV/EHU), Apartado 1072, 20080 San Sebastián, Spain ³Jülich Centre for Neutron Science JCNS, Forschungszentrum Jülich GmbH, Outstation at MLZ, Lichtenbergstraβe 1, 85747 Garching, Germany

⁴Laboratory for Neutron Scattering, Paul Scherrer Institut, CH-5232 Villigen, Switzerland ⁵Donostia International Physics Center, Paseo Manuel de Lardizabal 4, 20018 San Sebastián, Spain

kind of mixtures is also particularly interesting from a fundamental viewpoint due to the dynamic asymmetry characterizing the molecular mobilities of the components. 1–18 This refers to the markedly different characteristic times of the structural relaxations of the two kinds of molecules in the mixtures. A specially intriguing situation is that found for systems rich in the slow component. This vitrifies at higher temperatures than the minority component, leading to a range of temperatures where the fast molecules try to relax in a frozen environment. Mixtures of molecules presenting a hugely different mobility in their neat states can be found in such widely used materials as plasticized polymers—polymeric systems containing some amount of smaller (solvent) molecules.

solvent—in particular, in biological systems—has led to an enormous effort to characterize its properties in mixtures with different molecules. 19-23 An intriguing behavior has been reported for the dynamics of water molecules in concentrated solutions, namely, a change in the temperature dependence of the characteristic time from an Arrheniuslike law at low temperatures toward a stronger dependence that resembles a liquid-like Vogel-Fulcher behavior at high temperature.^{21,24–26} Some authors^{27,28} suggested a relation between such a crossover and the fragile-to-strong transition in water. However, in other works, 24 it was observed that the crossover occurred at the glass transition of the mixture, and so it could be related to a crossover from a situation where the surrounding medium would experience supercooled liquidlike dynamics toward a non-equilibrium situation where the solvent is confined in a rigid glassy environment. Below the glass-transition temperature, the motions of the water molecules are restricted by the frozen matrix and, therefore, are similar to a β -relaxation of a simple glass. Above the glass transition of the mixture, the water reorientation is coupled with the α -relaxation of the matrix. Consequently, the observed crossover could be interpreted as a transition from a local-like dynamics to a cooperative-like dynamics. On the other hand, we note that a transition from an Arrhenius to a non-Arrhenius dependence on temperature has also been found in the water dynamics confined in MCM-41²⁷ and, also very recently, in carbon nanohorns.²⁹ These hosts do not exhibit any glass transition and, due to the nature of the host, there are not structural rearrangements. Therefore, only thermal energy could contribute to the crossover. The origin of this phenomenon is thus, up to date, still controversial. Another interesting related question is whether or not such a crossover is also found in other solvent molecules displaying different interactions among them and with the confining

Within this framework, we have started a project consisting of a comparative study of the component dynamics in binary mixtures of a given polymer and either water or tetrahydrofuran (THF) as solvents. These two molecules interact through very different ways: H-bonding is the most relevant interaction for water, while THF molecules interact via van der Waals forces. Our interest was twofold: to determine the solvent effects on the polymeric matrix and to follow the confined solvent behavior. Regarding this question, we wanted first to see whether the above mentioned crossover is present in the dynamics of the solvents. If so, we wanted to characterize the properties of this phenomenon for both kinds of molecules in a comparative way. As polymeric matrix we have chosen poly(2-(dimethylamino)ethyl methacrylate) (PDMAEMA). This polymer is soluble in both solvents and displays a glass-transition temperature at about RT. This value is appropriate for our investigations since it is high enough to lead to mixtures with pronounced dynamic asymmetry and, at the same time, low enough to investigate the polymer dynamics in a wide temperature range without solvent evaporation problems. From an applied point of view, PDMAEMA is of interest for the development of materials with antibacterial properties³⁰ and used in gene therapy for its chemical properties.31

In two recently published works we have already investigated the component dynamics of THF mixtures with solvent concentration in weight $c^{THF}=30$ wt. %, corresponding to one THF molecule/monomer. 32,33 In those works, the dynamic study combined dielectric spectroscopy and quasielastic neutron scattering (QENS) on selectively deuterated samples in order to characterize the two components separately and provide spatial information on the molecular motions involved in the different processes. In Ref. 32 the polymer dynamics in a mixture with 30 wt. % of water was also investigated. A heterogeneous distribution of water molecules in the polymer—likely associated to the possible presence of water clusters—was invoked to explain the observed behavior. No experimental evidence for the existence of those clusters was provided though.

With the present work we complete this investigation. Here we address the structural and dynamical features of THF and aqueous mixtures of PDMAEMA covering a wide range of compositions (limited by crystallization at high solvent concentrations). To investigate the structure, we have combined X-ray diffraction, neutron diffraction with polarization analysis, and small angle neutron scattering. The dynamics have been studied by differential scanning calorimetry (DSC) and broad-band dielectric spectroscopy (DS). The paper is structured as follows: after the experimental section, we present the calorimetric results in order to know the locations of the glass transition temperatures (T_g) in the different samples. Then, the structural study is presented. There, we provide the experimental proof of water clusters, already from rather low water concentrations, while a homogeneous dispersion of the THF molecules is observed up to high solvent contents. Moreover, we show that a nano-phase separation of main-chain and side-group atoms of the polymer matrix persist in both kinds of mixtures. Then we move to describe our findings about the dynamical features. Most of them result from the dielectric study. Therefore, we first explain what are the main contributions to the dielectric permittivity in both kinds of mixtures and how they are analyzed. In the aqueous mixtures, the DS signal is overwhelmed by the water contribution, but in the THF mixtures the α and β -processes of the polymer can be followed, together with a contribution from the THF component. Then we describe and discuss the results on the different dynamical processes identified. We start with the polymer dynamics. The THF mixtures show a remarkable reduction of T_g and a "stronger" behavior of the α -relaxation of PDMAEMA even at the lowest THF concentration investigated (15 wt. %). The shift increases with the amount of THF but seems to saturate at $c^{THF} = 40$ wt. % where presumably some THF molecules start to interact mainly with each other. The DSC results on the aqueous systems evidence a strikingly broad glass-transition feature, revealing a highly heterogeneous behavior in accord to the structural study. Moving to the β -process of the polymer only accessible for the THF mixtures—it shows a markedly lower activation energy than that found in the dry sample already at $c^{THF} = 15$ wt. %, and the results support the scenario of a hindered slow component of the β -process proposed in the previous study of the 30 wt. %-composition.³² Finally,



the solvent dynamics are scrutinized. An analysis of the apparent activation energy of the water dynamics reveals a crossover toward a more pronounced temperature dependence than that dictated by the Arrhenius law characteristic of the glassy state, which takes place at the onset temperature of the glass-transition process in all the samples studied. Such finding puts forward the relevance of matrix mobility on the origin of the crossover in water dynamics when confined in this kind of systems. The crossover cannot be found in the dynamical process of the THF molecules, even at the highest THF concentrations. This absence is attributed to the lack of cooperativity effects in the relaxation of these molecules.

II. EXPERIMENTAL

A. Samples

PDMAEMA (see chemical formula in Fig. 1) was purchased from Polymer Source. The average molecular weight of the polymer is $M_w = 57\,000$ g/mol, with polydispersity $M_w/M_n = 3.0$. PDMAEMA as received was annealed for 7 h at T = 373 K under vacuum (primary vacuum $\approx 10^{-1}$ Torr) to evaporate possible trapped solvent. Mixtures with THF (solvent concentration in weight $c^{THF} = 15$, 20, 30, 40, and 48 wt.%) and with water (solvent concentration $c^{H_2O} = 20$, 30, 40 wt.%) were prepared by mixing the dry polymer with the appropriate amount of solvent during a few days. The same protocol was used to prepare the mixture with heavy water with $c^{D_2O} = 30$ wt.% investigated in the neutron diffraction experiments.

B. Diffraction

The structural features of the samples were investigated by X-ray (XR) and neutron diffraction. XR measurements were performed with a Rigaku equipment with a two-dimensional multiwire X-Ray Detector (Gabriel design, 2D-200X) of 200 mm diameter active area with ca. 200 μ m resolution. The azimuthally averaged scattered intensities were obtained as a function of scattering vector $Q = 4\pi \sin(\theta)/\lambda$, where θ is half the scattering angle and $\lambda = 1.54$ Å from Cu K- α

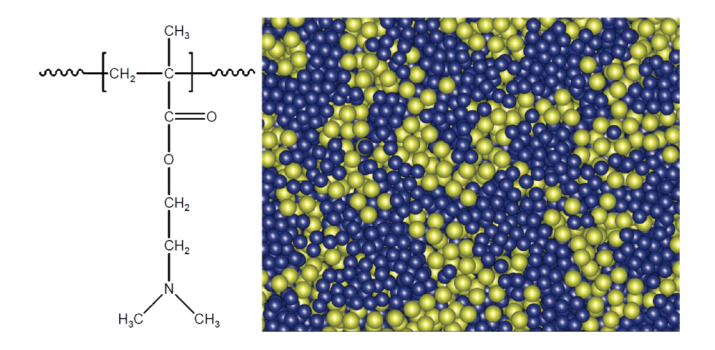


FIG. 1. Left: Chemical formula of PDMAEMA. Right: snapshot of the coarse-grained molecular dynamics simulations in comb-like polymers presented in Ref. 34 illustrating the nano-phase separation scenario for polymeric systems with long side groups. Bigger yellow beads represent coarse-grained molecular groups along the main-chain and smaller blue beads along the side groups.

transition photons. Measurements were performed under vacuum and in transmission geometry. The mixtures were sandwiched between mica windows and sealed to avoid solvent evaporation, while the dry sample was prepared as a film. Due to mica reflections at higher Qs, the Q-range under investigation was restricted below 1.2 Å⁻¹. The patterns were collected at different temperatures between -120 and 20 °C.

The neutron scattering investigation was performed on the dry polymer and a sample with 30 wt. % deuterated water. Heavy water was used in order to achieve a large contrast between the components. Measurements were carried out by using the DNS instrument at the Forschungs-Neutronenquelle Heinz Maier-Leibnitz in Garching (Germany) allowing polarization analysis. An incident neutron wavelength of $\lambda = 4.2 \text{ Å}$ was used covering a Q-range from $Q = 0.2 \text{ Å}^{-1}$ to $Q = 2.67 \text{ Å}^{-1}$. Four different temperatures were investigated in the range 180 K $\leq T \leq$ 280 K. Background correction was done by subtracting the intensity scattered by an empty aluminum sample holder. In order to extend the investigation toward lower Q-values, small-angle neutron scattering measurements were performed by means of SANS-2 instrument at SINQ, Paul Scherrer Institute in Villigen (Switzerland). A wavelength of 7.5 Å was used with a sampledetector distance of 1.2 m. Room temperature conditions were investigated.

C. Dielectric spectroscopy and differential scanning calorimetry

Broadband dielectric spectrometer Novocontrol Alpha-S was used to measure the complex dielectric function $\epsilon^*(\omega)$ = $\epsilon'(\omega) - i\epsilon''(\omega)$, covering a frequency range of $f = (\omega/2\pi)$ = 10^{-2} - 10^{7} Hz. The samples were prepared forming a parallelplate capacitor between parallel gold-plated electrodes with a diameter of 20 mm. Measurements were carried out under isothermal conditions every 5 K with a temperature stability better than 0.1 K. The maximum temperature for the dry polymer (370 K) was chosen to avoid degradation, while for the mixtures we performed measurements up to 300 K to prevent a significant solvent evaporation. Differential scanning calorimeter (DSC) TA Instrument Q2000 was used to determine the glass-transition temperature T_g of the samples (sample weights about 10 mg). Hermetic aluminum pans were used for all the samples. Modulated DSC measurements were performed with average heating rate of 3 K/min and amplitude of modulation ± 0.5 K with a period of $t_p = 60$ s.

III. CALORIMETRIC INFORMATION ABOUT THE GLASS TRANSITIONS

Figure 2 shows the normalized temperature derivative of the reversible part of the specific heat dC_p^{Rev}/dT during heating as function of temperature for all mixtures investigated in comparison with the dry system. This quantity provides a sensitive method to determine the glass-transitions—the location of a maximum in this function corresponds to the inflection point in the specific heat trace which is associated



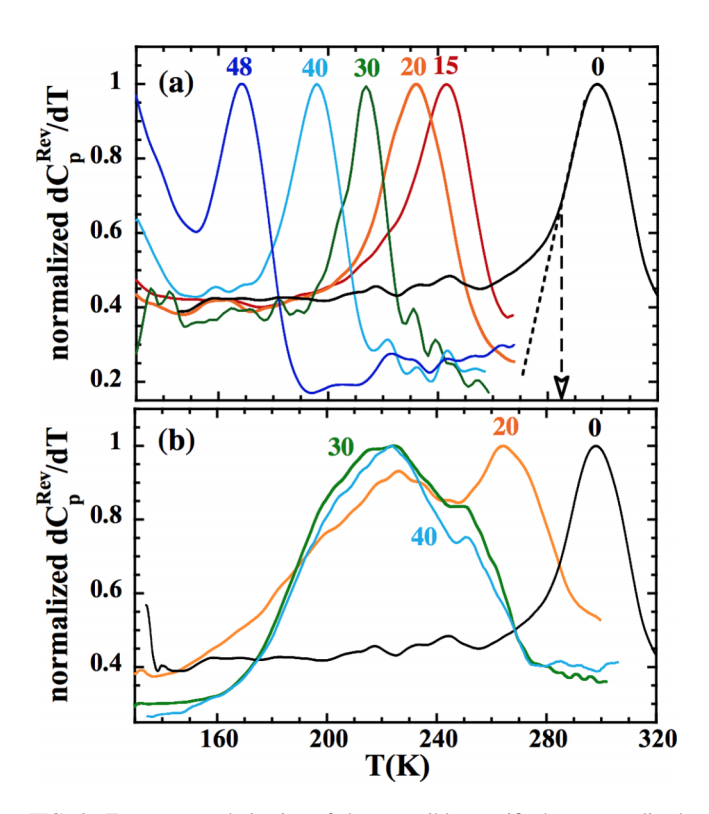


FIG. 2. Temperature derivative of the reversible specific heat normalized to its maximum value for PDMAEMA/THF (a) and PDMAEMA/H₂O (b) mixtures with the indicated solvent concentrations (wt. %). Dry polymer results are also shown for comparison (black curves). As an example, for dry PDMAEMA in (a) the dotted line shows the extrapolated linear description of the low-T flank of the glass-transition peak, and the dashed arrow the accordingly obtained location of the $T_{e,onset}^{DSC}$ -value.

to a given glass-transition process. We will denote as T_g^{DSC} the T_g -value obtained from the maximum of dC_p^{Rev}/dT . Figure 2 directly reveals a pronounced plasticization effect (decrease of the T_g -value) by addition of solvent. For instance, we note that adding only a small amount of THF ($c^{THF}=15$ wt. %), a shift of T_g^{DSC} by about 50 K is observed. Another interesting parameter is the onset of the glass-transition process $T_{g,onset}^{DSC}$, which can be determined from the temperature at which dC_p^{Rev}/dT deviates from the linear behavior defined by the low-temperature flank of the peak [see as an illustrative example the dotted line in the data of the dry system in Fig. 2(a)]. The values of T_g^{DSC} and $T_{g,onset}^{DSC}$ and are compiled in Tables I and II.

TABLE I. T_g -values determined from DSC and DS and parameters obtained by VF descriptions of the characteristic times of the α -relaxation of PDMAEMA in the dry state and at different THF concentrations by fixing the pre-factor to that obtained for the dry PDMAEMA $(\log[\tau_0(s)] = -11.7)$.

c wt. %	$T_g^{DSC}(\mathbf{K})$	$T_{g,onset}^{DSC}(K)$	$T_g^{DS}(\mathbf{K})$	B (K)	$T_0\left(\mathrm{K}\right)$
0	299 ± 1	285 ± 2	287 ± 1	1666 ± 6	230.8 ± 0.3
15	250 ± 1	230 ± 2	229 ± 1	1946 ± 21	165 ± 1
20	233 ± 1	215 ± 2	221 ± 1	2124 ± 38	152 ± 2
30	214 ± 1	200 ± 2	204 ± 1	1881 ± 6	142 ± 0.3
40	195 ± 1	175 ± 2	190 ± 1	1793 ± 17	135 ± 1
48	169 ± 1		189 ± 1	1821 ± 7	129.5 ± 0.4

TABLE II. Values of the glass transition temperatures (inflection point) and onset determined from DSC for the samples with different H₂O concentrations.

c wt. %	$T_g^{DSC}(\mathbf{K})$	$T_{g,onset}^{DSC}\left(\mathrm{K}\right)$	$T_{g,highT}^{DSC}(K)$
20	226 ± 4	180 ± 10	264 ± 3
30	221 ± 5	180 ± 5	
40	223 ± 4	180 ± 5	

An increasingly pronounced shift of the glass-transition temperature upon addition of THF molecules is observed, reflecting that the plasticization effect continuously increases with the solvent concentration. The difference between T_{σ}^{DSC} and $T_{g,onset}^{DSC}$ —representative for the width of the transition—is of about 20 K for all THF-concentrations, with exception of the mixture with $c^{THF} = 30$ wt. %. The glass-transition process in this sample spans over about 14 K, i.e., has the same width as the dry polymer. Finally, we mention that for PDMAEMA/THF with $c^{THF} = 48$ wt. %, a crystallization peak at around ~130 K is found on cooling. This prevents an accurate determination of the onset of the glass transition. For lower concentrations, no sign of THF crystallization is detected during cooling. However, the data for 40 wt. % THF concentration show a weak hint of melting in the low temperature region investigated [see Fig. 2(a)].

The aqueous systems also show plasticization; however, their DSC curves show strikingly different features from those of the THF mixtures. In particular, the widths of the glass-transition processes are much larger. Moreover, the peak position is hardly dependent of concentration for 30 wt. % and 40 wt. % water contents. For the lowest water concentration investigated, a clear bimodal structure of the curve can be seen. This sample exhibits thus two glass-transition processes, one at lower temperatures—roughly with the same characteristics of that observed for higher water concentrations—and another one at higher temperatures (about 265 K). Reminiscences of a second glass-transition process could also be envisaged for the $c^{\rm H_2O}=30$ wt. % and $c^{\rm H_2O}=40$ wt. % samples at about 250 K; however, the results cannot be considered as conclusive in this direction.

IV. STRUCTURAL FEATURES

The XR-diffraction results at 293 K are shown in Fig. 3. In the Q-region below 1 Å $^{-1}$ the main feature in the dry system is the presence of a peak centered at around ≈ 0.5 Å $^{-1}$. The position and width of this peak are not appreciably influenced by the presence of THF for concentrations $c^{THF} \leq 30$ wt. %, but higher amounts of this solvent lead to clear additionally scattered intensity in the low-Q flank of the peak. Contrarily, the effect of water starts to be notable already for the lowest concentration investigated. For $c^{H_2O} = 20$ wt. %, a relatively weak but clear bump appears in the low-Q flank of the peak. With increasing water concentration, this bump gradually develops leading to a clearly resolvable additional peak centered at $Q \approx 0.25$ Å $^{-1}$ for $c^{H_2O} = 40$ wt. %. Figure 4 displays the neutron diffraction



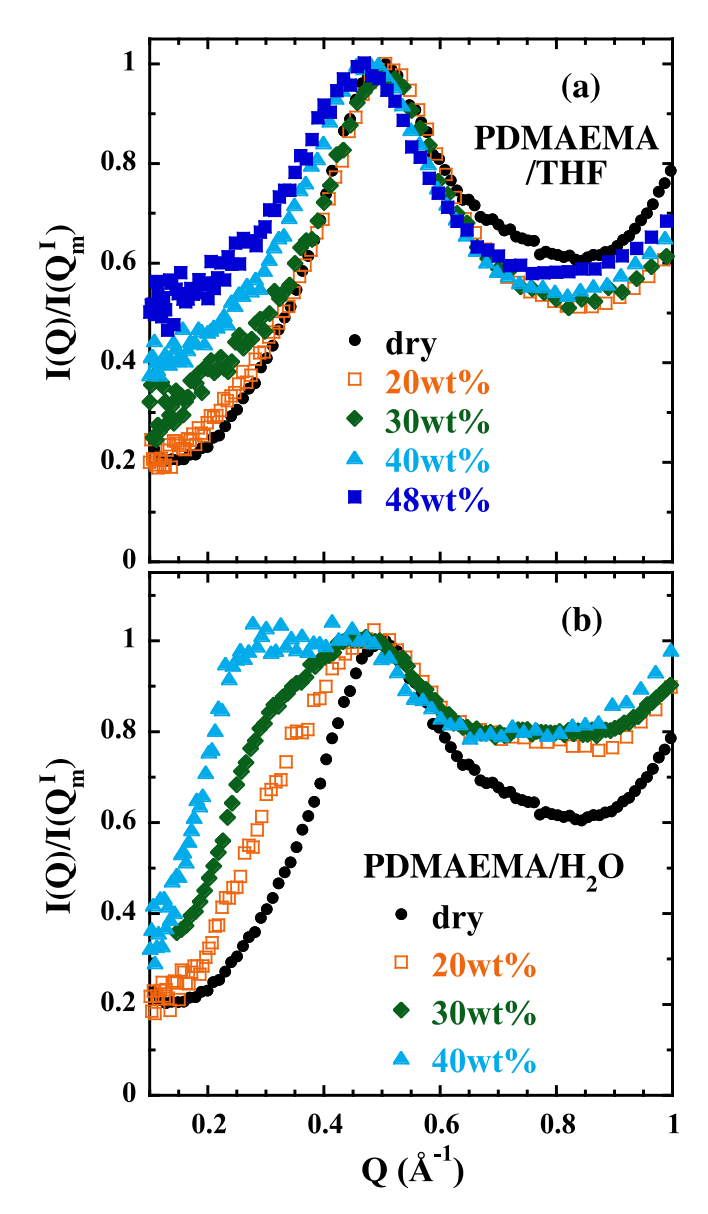


FIG. 3. XR-diffraction patterns obtained on THF-mixtures (a) and aqueous solutions (b) at 293 K, compared with the results on dry PDMAEMA. Data have been normalized to the intensity at $Q_m^I \approx 0.5 \ \text{Å}^{-1}$.

results. The neutron intensity coherently scattered by the mixture PDMAEMA/D₂O [Fig. 4(a)] is dominated by a strong peak at low-Q values (centered in the range 0.2–0.25 Å⁻¹). At the two lowest temperatures investigated (180 and 220 K), the intensity and the position of the peak maximum are similar. Increasing the temperature, the intensity increases and the maximum shifts toward lower Q values, getting out of the DNS window close to room temperature. The presence of such a peak is confirmed by the SANS results at RT shown in Fig. 4(b).

In addition to the main peak, the DNS results on the mixture reveal signatures of a weak maximum at around $0.5\text{-}0.6\text{Å}^{-1}$ —also visible in the dry sample pattern—and an enhancement of the correlations with respect to those in the dry state in the *Q*-range around 1.5 Å⁻¹ [Fig. 4(a)]. This feature becomes even more marked at lower temperatures. In the following, we address the origin of the diffraction peaks

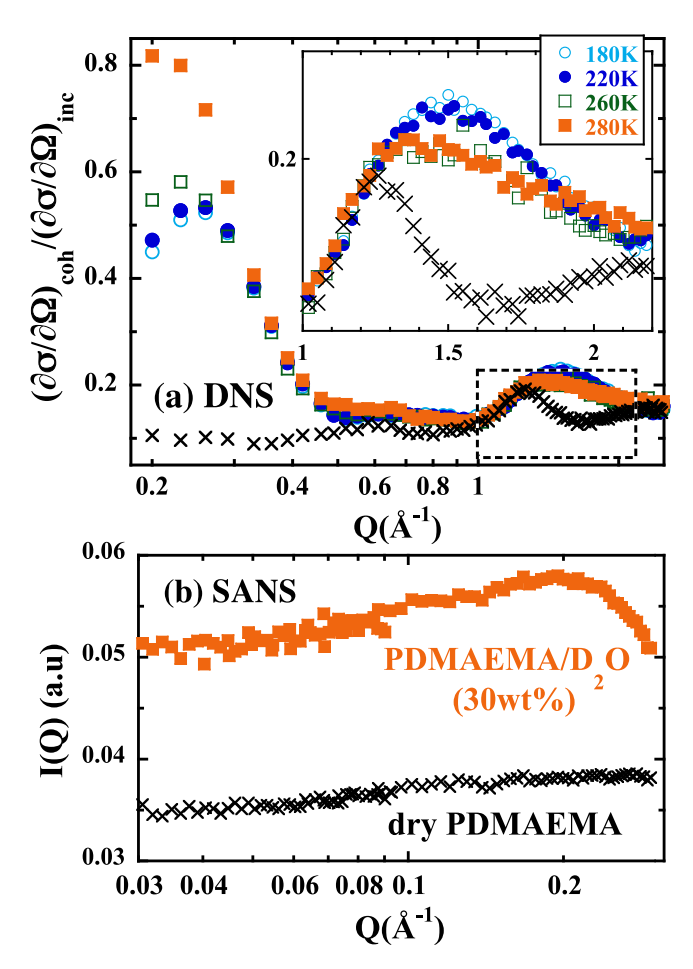


FIG. 4. (a) Ratio between the coherent and incoherent scattering cross sections measured by DNS on PDMAEMA/D₂O with $c^{\mathrm{D_2O}}=30$ wt. % at the different temperatures indicated. Crosses show the dry PDMAEMA results at 280 K. The inset shows a magnification (with linear abscissa scale) of the area marked with the dashed rectangle. (b) SANS results on PDMAEMA/D₂O with $c^{\mathrm{D_2O}}=30$ wt. % (squares) and dry PDMAEMA (crosses) at RT.

and try to provide a consistent picture of the structural features in the samples investigated.

Figures 3 and 4(a) show that the structure factor of dry PDMAEMA presents two main maxima in the region below $Q \le 2 \text{ Å}^{-1}$, namely, centered at $Q_m^I \approx 0.5 \text{ Å}^{-1}$ ("peak I") and $Q_m^{II} \approx 1.2 \text{ Å}^{-1}$ ("peak II"). Due to the complex molecular composition of PDMAEMA monomer (see Fig. 1), attributing these features to specific correlations between molecular groups is not an easy task. However, comparing the results with those on similar polymers investigated by diffraction and molecular dynamics simulations in previous works, it is possible to provide a picture for the main structural features of PDMAEMA. We note the qualitative—and even semi-quantitative—similarity of its pattern with those reported for other polymers also containing long and/or relatively bulky side-groups, i.e., polymers of the family of poly(n-alkyl methacrylates),³⁵ poly(n-alkyl acrylates),³⁶ poly(itaconates),³⁷ poly(alkylene oxides),³⁸ polystyrene,³⁹ poly(vinyl pyrrolidone),⁴⁰ and some poly(methyl methacrylate)-based polyelectrolytes.⁴¹ Those systems also display a "pre-peak" (peak I) at low Q and a main peak at around $\sim 1.2 \text{ Å}^{-1}$. The presence of peak I has been attributed to a kind of nano-phase segregation



between side groups and backbones leading to the existence of nano-domains rich in each of the polymeric subspecies. 36,42,43 Such scenario was supported by coarse-grained simulations on generic comb-like polymers, 34 as can be seen in the simulation snapshot reproduced in Fig. 1. Peak I would be related to inter-domain correlations. 34 In this context, the deduced value for the average domain size for PDMAEMA is about $d_I = 2\pi/Q_m^I \sim 12$ Å. Also within this scenario, peak II has usually been assigned to correlations between atoms belonging to side groups of different monomers within the nano-domain. In PDMAEMA it reveals atomic pair correlations with an average distance of about $d_{II} = 2\pi/Q_m^{II} = 5.3$ Å.

Adding THF does not qualitatively change the features of peak I, as can be appreciated in Fig. 3. The presence of a unique maximum in the region $Q \le 0.7 \text{ Å}^{-1}$ in a similar position as in the dry sample indicates that the nano-domain structure remains practically unchanged upon THF inclusion up to concentrations of about 30 wt. % (i.e., about one THF molecule/monomer). At higher THF concentrations, the situation is qualitatively unaltered. However, the increased scattered intensity in the low-Q flank of peak I and the slight shift of this maximum towards lower Q-values suggest the appearance of nano-domains with larger sizes than those existing in the dry polymer (or in the mixtures with lower THF concentrations) and the subsequent increase of the average size of the nano-domains. These results can be interpreted as follows: For concentrations smaller or equal to one THF molecule/monomer, THF molecules are homogeneously distributed around in the sample. They can be uniformly accommodated within the nano-domains, occupying sites homogeneously scattered around the sample and without appreciably distorting the nano-domain structure. The decrease of the intensity in the minimum between peaks I and II with respect to the intensity at Q_m^I could probably be related to the presence of THF molecules in the interstices between PDMAEMA side groups, leading to negative contributions of cross-correlations in this Q-region. This situation leads to saturation at the 30 wt. % concentration. Adding more solvent, some PDMAEMA main-chains have to separate from each other in order to increase the space between them and put up more THF molecules in the side-group nano-domain. This effect manifests itself by the increased scattered intensity at low Q and naturally becomes more pronounced with increasing THF concentration. We note that accompanying this effect a kind of partial segregation of the THF molecules is expected. Interactions would appear between solvent molecules accommodated very close to each other within the expanded nano-domains. These molecules are expected to behave in a different way than those finding an environment mainly consisting of polymeric sidegroups, as those THF molecules present in the samples with $c^{THF} \leq 30 \text{ wt. } \%.$

The situation in the hydrated sample is markedly different. Peak I is still present in the region $\approx 0.5~\text{Å}^{-1}$ in both, XR and neutron patterns [see Figs. 3(b) and 4], suggesting the persistence of the nano-domain structure in the polymeric matrix with similar or slightly increased associated nano-domain sizes with respect to the dry sample, within the uncertainties. However, a new peak appears in the patterns in

the *Q*-region $\approx 0.25 \text{ Å}^{-1}$. The intensity of this peak increases with H₂O concentration and is particularly prominent in the neutron diffraction data (see Fig. 4). The large difference between deuterium and proton scattering lengths for this probe induces a large contrast between molecules containing deuterated and protonated nuclei. The intense peak found in the low-Q range of the DNS results can therefore be attributed to the presence of regions rich in deuterated water dispersed all over the sample, giving rise to a well defined correlation distance. The Q-values of the peak maximum correspond to large average correlation distances in the range of 25 < d < 31 Å, i.e., much larger than the typical nano-domain size in PDMAEMA. The tendency of water molecules to form clusters, i.e., to join together instead of being uniformly distributed in the sample is well known. Therefore, it would be reasonable to relate this scattering contribution to the presence of water clusters, and thereby the deduced characteristic spatial length to the average distance between them. Contrarily, the presence of THF clusters cannot be inferred from the structural results here presented; neutron diffraction experiments on labelled samples with 30 wt. % THF-concentration presented in Ref. 33 also ruled out their formation in a PDMAEMA matrix. However, after the above discussion, increasing the THF concentration above one molecule/monomer, we could expect the appearance of regions with enhanced THF/THF interactions scattered around the sample.

Considering now the thermal evolution of the patterns in the region of peak I (Fig. 5), for THF mixtures we can observe a gradual increase of the intensity of this peak and a very slight shift towards lower Q-values (equivalently larger distances) with increasing temperature, which could be attributed to thermal expansion of the nano-domains. The results on the aqueous solutions reveal a more complex situation. The shift of the global maximum around 0.5 Å⁻¹ for the 20 wt. % water concentration sample to higher Q-values when heating suggests the interplay of different correlations in this region including those characteristic for the nano-domain structure which are able to evolve at high temperature. Particularly remarkable are the changes in the structure factor of the 40 wt. % water concentration sample above its glass transition, suggesting an intricated superposition of different correlations in this Q-region.

At higher Q-values $(1 \le Q \le 2 \text{ Å}^{-1})$, a broad peak is found in the diffraction data of the aqueous mixture [see Fig. 4(a)]. The direct comparison with the dry results suggests that its main contribution should be attributed to correlations involving deuterated water nuclei. The shape of such a peak appears highly dependent on the temperature range. At high temperature it is centered at around 1.2 Å⁻¹ and characterized by a strong asymmetry, whereas at the two lowest temperatures investigated (180 and 220 K), the peak appears more symmetric and the maximum is shifted toward higher Q-values. We note that very similar qualitative features and temperature dependence have been reported for water confined in mesoporous MCM-41.44,45 A combined study of neutron diffraction and empirical potential structure refinement (EPSR) simulations⁴⁵ suggested that the mesoscopic arrangement of water molecules in the pore could



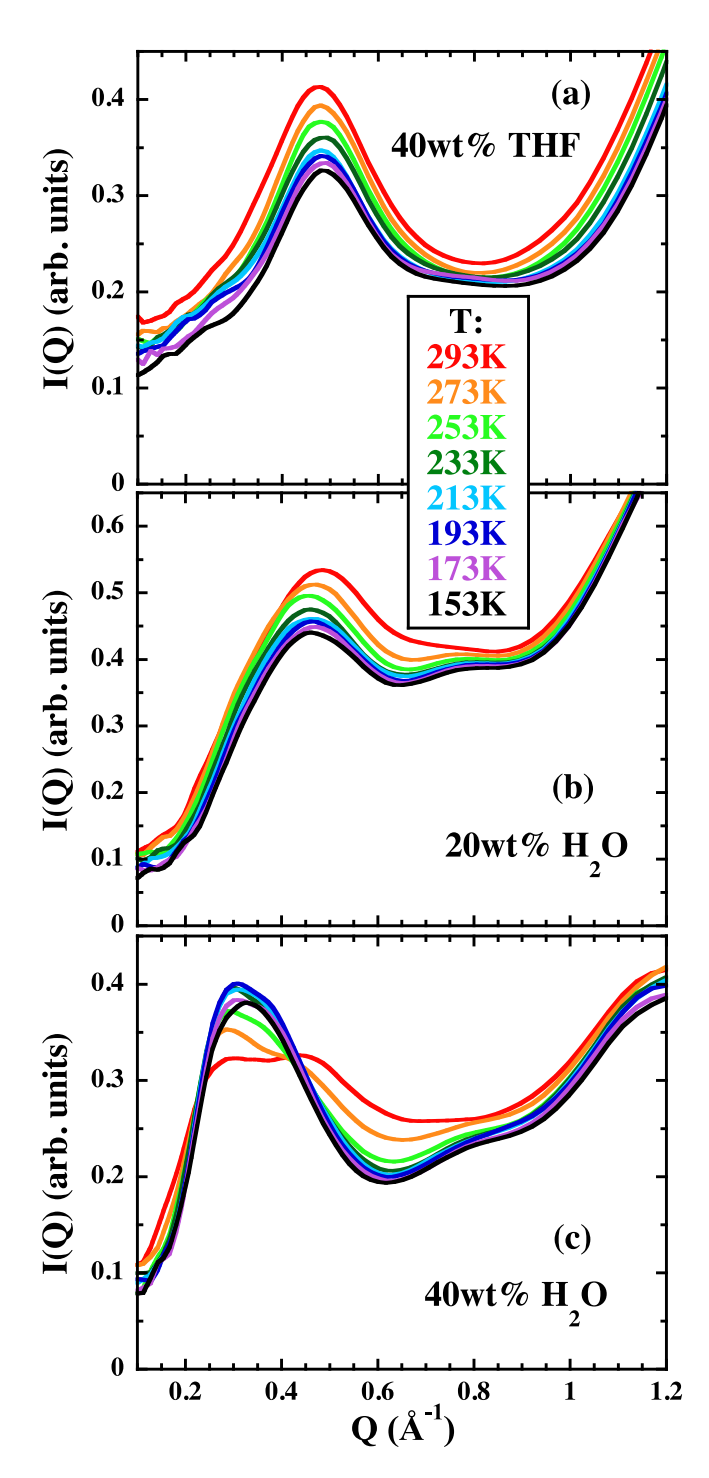


FIG. 5. Temperature evolution of the XR-diffraction results on the sample with $c^{THF}=40$ wt. % (a), $c^{H_2O}=20$ wt. % (b), and $c^{H_2O}=40$ wt. % (c), with the common temperature color code indicated. Data have been smoothed for clarity.

change as a result of the modified water-water and water-substrate interactions. Upon cooling, the H-bonds between water molecules would be strengthened, while those between water and the wall atoms become weaker. Therefore, at low temperature the pore would appear more uniformly filled while the walls are less wet and water molecules are arranged in a cubic-ice-like structure. The analogies found between the patterns of the two systems suggest that the features observed for the structure factor at $Q \approx 1.5 \text{ Å}^{-1}$ are related

in our case to intra-cluster organization of water molecules within the polymeric matrix. This means, such molecular reorganization would not be directly connected to the above described structural evolution at the inter-cluster and polymer nano-domains levels.

V. DYNAMICAL FEATURES

A. Processes resolved by broadband dielectric spectroscopy

1. THF-mixtures

Due to large conductivity contributions it is not possible to clearly resolve the high-temperature process related to the structural relaxation of PDMAEMA in $\epsilon''(\omega)$. Therefore, the analysis of the dielectric α -process of the polymer was carried out on the real part of $\epsilon^*(\omega)$, $\epsilon'(\omega)$, where DC-conductivity does not contribute. In particular, we considered the derivative of $\epsilon'(\omega)$ with respect to $\log(\omega)$, $\partial \epsilon'(\omega)/\partial \log(\omega)$, since this function exhibits a maximum at a similar frequency as the $\epsilon''(\omega)$ relaxational counterpart. As an example, Fig. 6 shows $\partial \epsilon'(\omega)/\partial \log(\omega)$ for representative concentrations at T=250 K.

The contribution of the polymer α -relaxation was described in terms of the usually invoked Havriliak-Negami function

$$\epsilon^*(\omega) = \epsilon'(\omega) - i\epsilon''(\omega) = \epsilon_{\infty} + \frac{\Delta \epsilon}{[1 + (i\omega \tau_{HN})^{\alpha}]^{\beta}}.$$
 (1)

Here, α and β are shape parameters and τ_{HN} the characteristic time. Accordingly, the data were fitted by the corresponding expression

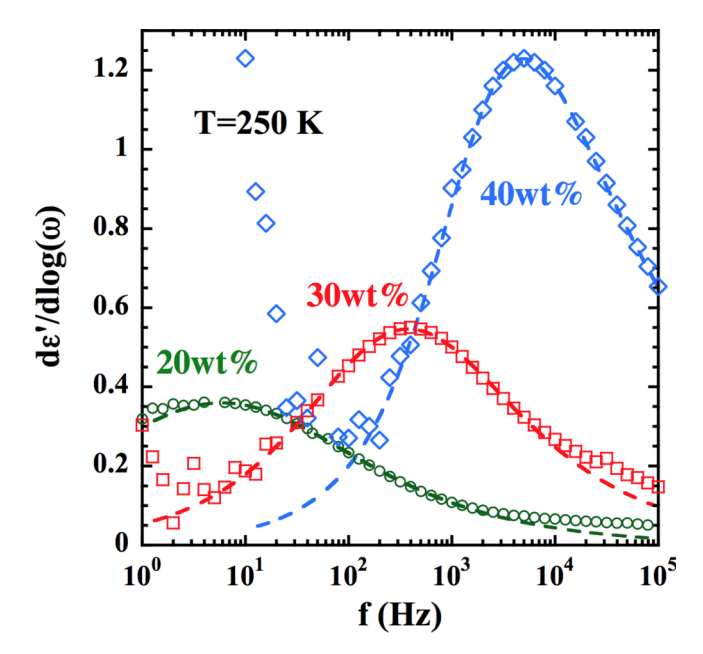


FIG. 6. Derivative of $\epsilon'(\omega)$ with respect to $\log(\omega)$ at T=250 K of PDMAEMA/THF with c=20, 30, and 40 wt. %. The process giving rise to the peak is the α -relaxation of the polymer. Dotted lines show the fits with Eq. (2).



$$\frac{\partial \epsilon'(\omega)}{\partial \log \omega} \propto \Re \left[\frac{(i\omega \tau_{HN})^{\alpha}}{[1 + (i\omega \tau_{HN})^{\alpha}]^{\beta+1}} \right]. \tag{2}$$

The good quality of the fits is shown in Fig. 6. The characteristic time τ_{max} —defined as the inverse of the frequency ω_{max} at the $\epsilon''(\omega)$ -peak—was then calculated using the relationship⁴⁶

$$\tau_{max} = \tau_{HN} \left[\frac{\sin(\frac{\alpha\beta\pi}{2+2\beta})}{\sin(\frac{\alpha\pi}{2+2\beta})} \right]^{1/\alpha}.$$
 (3)

Moving now to the glassy state, Fig. 7 shows the imaginary part of the dielectric response of PDMAEMA/THF at selected temperatures. At low concentration two peaks are well resolved. The intensity of the low-frequency loss peak increases with THF concentration, suggesting motions of solvent molecules as its main origin. At high THF concentration this process almost covers the high-frequency peak. Considering the location and expected strength of the contribution of the β -relaxation of the polymer to the dielectric response, this high-frequency contribution could be attributed to the β -relaxation of the polymer, modified by the presence of solvent. The validity of such hypothesis was proved by quasielastic neutron scattering experiments for the sample with 30 wt. % THF-concentration. 32

To describe these relaxational processes symmetric Cole-Cole (CC) functions were used⁴⁶

$$\epsilon_{cc}^*(\omega) = \epsilon_{\infty} + \frac{\Delta \epsilon}{[1 + (i\omega \tau_{cc})^{\alpha_{cc}}]},$$
 (4)

with τ_{cc} ($\equiv \tau_{max}$) the Cole-Cole characteristic relaxation time and α_{cc} the shape parameter. The data were fitted to the sum of two CC functions, taking into account both the polymer and the THF contributions above identified.

2. H₂O-mixtures

Due to the high conductivity contribution, it is not possible to resolve the dielectric signature of the PDMAEMA structural relaxation. At lower temperatures, only one process is detected. Figure 8 shows the loss tangent $\tan(\delta) = \epsilon''(\omega)/\epsilon'(\omega)$ of the dielectric response at T=160 K. The intensity of this peak is much more intense than those displayed by dry PDMAEMA and increases with water concentration. This symmetric peak could be well described by a CC function.

B. Polymer dynamics

1. Segmental relaxation

For the THF-mixtures, detailed information about the segmental polymer dynamics related with the glass-transition phenomenon was obtained from the dielectric study. The deduced values of τ_{max} for this process are presented in Fig. 9.

These times clearly show a Vogel-Fulcher (VF) temperature dependence,

$$\tau = \tau_0 \exp\left(\frac{B}{T - T_0}\right). \tag{5}$$

Here, τ_0 is a prefactor with the meaning of an inverse attempt frequency, B is an activation term and T_0 is the so-called

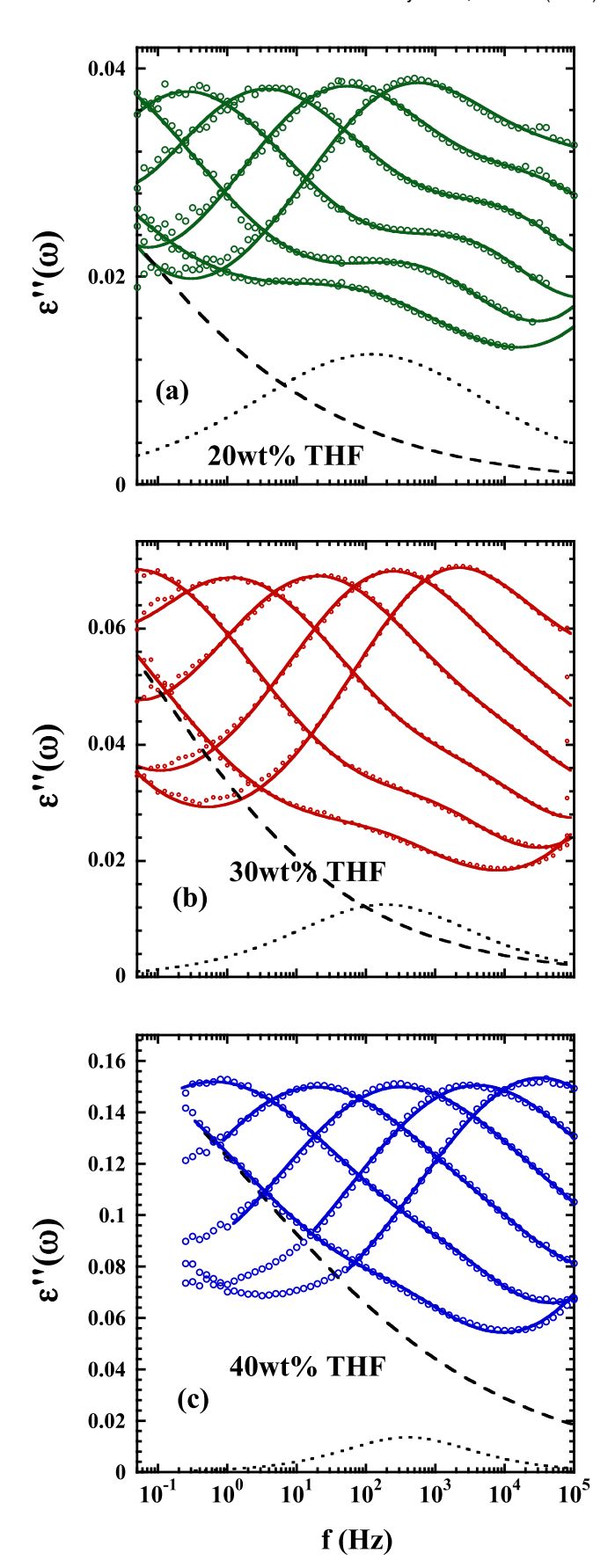


FIG. 7. Imaginary part of the complex dielectric permittivity at different temperatures below T_g : (a) PDMAEMA/THF 20 wt. %; (b) PDMAEMA/THF 30 wt. %; and (c) PDMAEMA/THF 40 wt. %. Continuous lines show the fit curves, while dashed (dotted) line represents the THF (PDMAEMA β -relaxation) component at the lowest temperature.

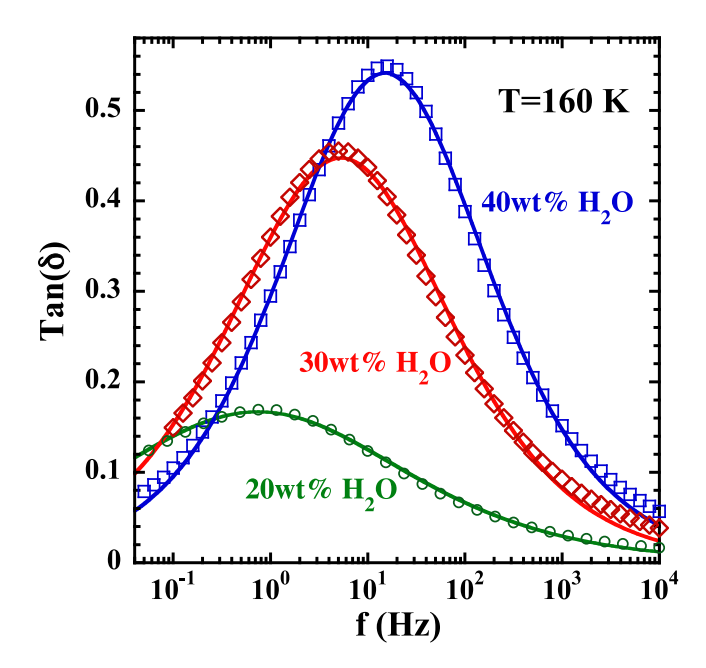


FIG. 8. ${\rm Tan}(\delta)$ of the complex dielectric permittivity of PDMAEMA aqueous mixtures at $T=160~{\rm K}$ and different water concentrations: 20 wt. % (green circles), 30 wt. % (red diamonds), and 40 wt. % (blue squares). Lines are Cole-Cole fits.

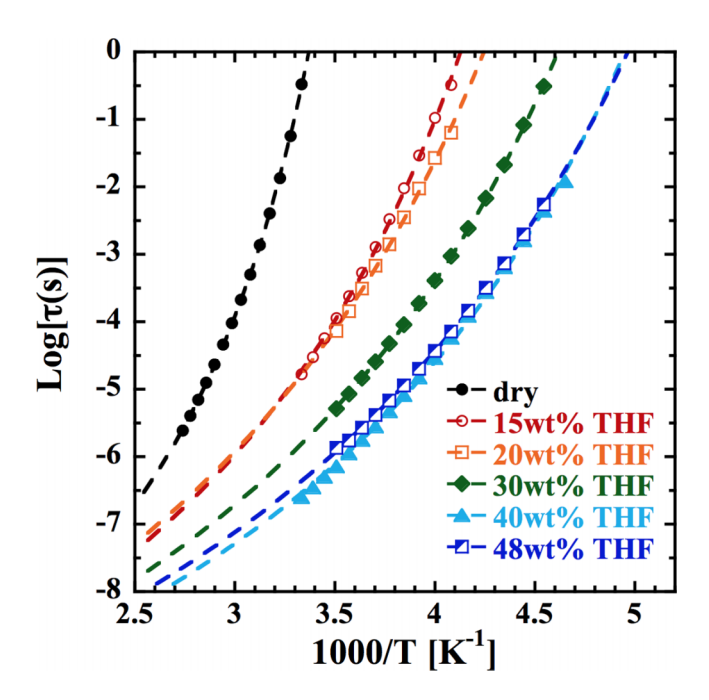


FIG. 9. Inverse temperature dependence of the characteristic times of PDMAEMA α -relaxations in the dry state and at different THF concentrations obtained by DS. Dashed lines are fits with VF expression.

VF-temperature at which the characteristic time would diverge. Very similar VF prefactors τ_0 are obtained for the different samples. Therefore, assuming that such parameter does not depend on the THF amount, the curves in Fig. 9 were obtained by Eq. (5) with a common prefactor $\log[\tau_0(s)] = -11.7$. The such deduced VF parameters B and T_0 are included in Table I.

We may define the dielectric spectroscopy temperature of glass transition (T_g^{DS}) as the temperature at which the relaxation time determined by this technique is $\tau = 100$ s. Based on this

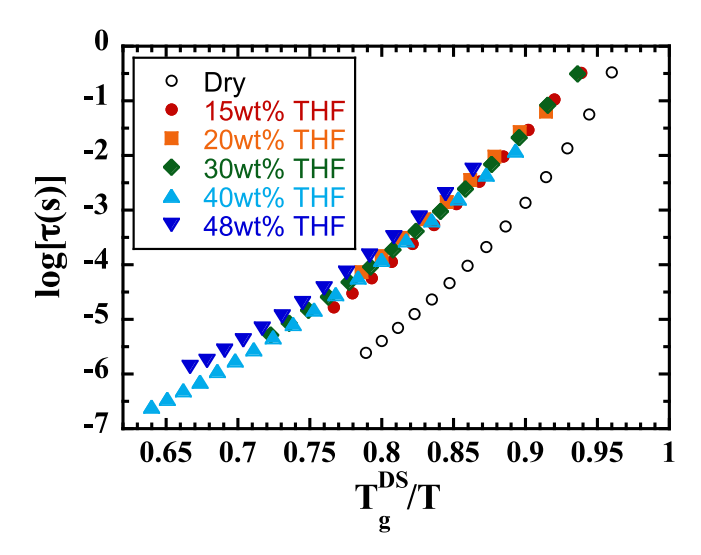


FIG. 10. Relaxation times of the polymer α -relaxation as function of the temperature scaled by the dielectric T_g (Angell's representation). Empty symbols refer to PDMAEMA in the dry state, while filled symbols represent the characteristic times in THF mixtures: $c^{THF}=15$ wt. % (red circles), 20 wt.% (oranges squares), 30 wt.% (green diamonds), 40 wt.% (light blue triangles), and 48 wt.% (dark blue down triangles).

definition, Fig. 10 shows an Angell's plot $(\log(\tau_{max}) \text{ vs } T_g^{DS}/T)$ of the results obtained at different concentrations. Samples with THF show a "stronger" behavior (less curved) than the sample in the dry state. Data corresponding to the different THF mixtures collapse on the very same curve. This result was not expected *a priori* and suggests that the effect of solvent on fragility, once it is induced already at relatively small concentrations (≤ 15 wt. % in the case of this system), does not essentially depend on concentration. Whether this is a general effect in plasticized polymers and its origin will be subject of future investigations.

The decrease of $T_g^{\widetilde{DS}}$ with increasing THF concentration takes place monotonically, in a similar way as observed by DSC up to $c^{THF} = 30$ wt. %. At the highest concentrations, the dielectric results point to a less pronounced concentration dependence of the glass transition. This could be understood taking into account that DSC is sensitive to both components in the mixtures. While at low THF concentrations the calorimetric signal is dominated by the polymer contribution (that is by far the main component of the mixture), for higher solvent concentrations THF is also significantly contributing. We also notice that the relaxation times of the highest concentration (48 wt. %) are very similar to those obtained for PDMAEMA/THF 40 wt. %, leading to the same T_a^{DS} , within the uncertainties. This could indicate that beyond a given concentration in the range 40-48 wt. %, any added THF molecule does not affect the polymer segmental dynamics at least as monitored by DS-anymore. We will see that the inferred partial segregation of THF molecules at this high concentration has impact also in other dynamical features.

For the hydrated samples, polymer dynamics are not accessible by DS but the information is extracted from the DSC results. The glass-transition features revealed by calorimetry are very different from those in the THF mixtures (see Fig. 2 and Tables I and II). First, the broadening of the main process



is extremely pronounced ($T_g^{DSC} - T_{g,onset}^{DSC} \approx 45$ K). This should be a consequence of extremely heterogeneous environments for polymer segments in the water mixtures. Second, the lower glass-transition temperature value of ≈225 K is rather insensitive to water concentration. This glass-transition temperature might be interpreted as that corresponding to the most probable local composition in the mixtures. We note that this T_o^{DSC} -value is similar to that observed for the THF-mixture with $c^{THF} = 30$ wt. %, i.e., one THF molecule/monomer. Following the above discussion, the homogeneous distribution deduced for the THF molecules in PDMAEMA implies that for such concentration all monomers are affected by the close proximity of one THF molecule. Apparently, the effect on the polymer dynamics by water molecules in such most probable composition regions is similar to that caused by one THF molecule. Finally, the clear bimodal character of the curve at the lowest water concentration investigated points to the presence of specially poorly hydrated regions in this mixture, reflecting probably a situation of phase separation.

2. B-Relaxation

In a previous work focused on the $c^{THF} = 30$ wt. % sample,³² DS and quasielastic neutron scattering (QENS) techniques were applied. The synergetic analysis of DS and QENS results on dry PDMAEMA and its mixture with THF suggested two kinds of side-group molecular motions—a slow and a fast one—contributing to the β -process of the polymer in the dry state. Based on the spatial information provided by QENS, a model for the geometry of the motions involved in the fast process was proposed. They would involve the side group and be spatially confined. For the methylene hydrogens, the motion would be restricted within a disc of about 3 Å of radius. The side-group methyl-group hydrogens would also participate in this process—in addition to rotate. In this case, the dimension of the disc defining the local motion would be determined by the distance between the centers of mass of the methyl groups, namely, 3.3 Å. Upon addition of solvent, this process would remain essentially unaltered, while the population involved in the slower one would be reduced. With the present investigation considering a wide range of THF concentrations, we aim to check the consistency of the proposed scenario for the polymer β -process.

For all THF mixtures investigated, the β -process associated to the polymeric component displays similar features, which clearly differ from those in the dry state: (i) a strong decrease of the dielectric strength of this process as soon as THF-solvent is added, even at the lowest concentration investigated. Within uncertainties, the relaxation strength $\Delta \epsilon$ in the mixtures is independent on temperature and proportional to the polymer concentration: i.e., $\Delta \epsilon \approx 0.05(1 - c^{THF})$ whereas in the dry state $\Delta \epsilon \approx 0.13$. This shows that the dielectric strength in the mixtures remains always weaker than expected by a factor close to 3 (ii) a clear narrowing is observed for the loss peak, evidenced by the higher values of the α_{cc} parameter in the mixtures, since we found $\alpha_{cc} = 0.45 - 0.47$ in the mixtures whereas $\alpha_{\rm cc} = 0.25 - 0.30$ in the dry polymer (iii) the characteristic times exhibit a markedly weaker temperature dependence [see

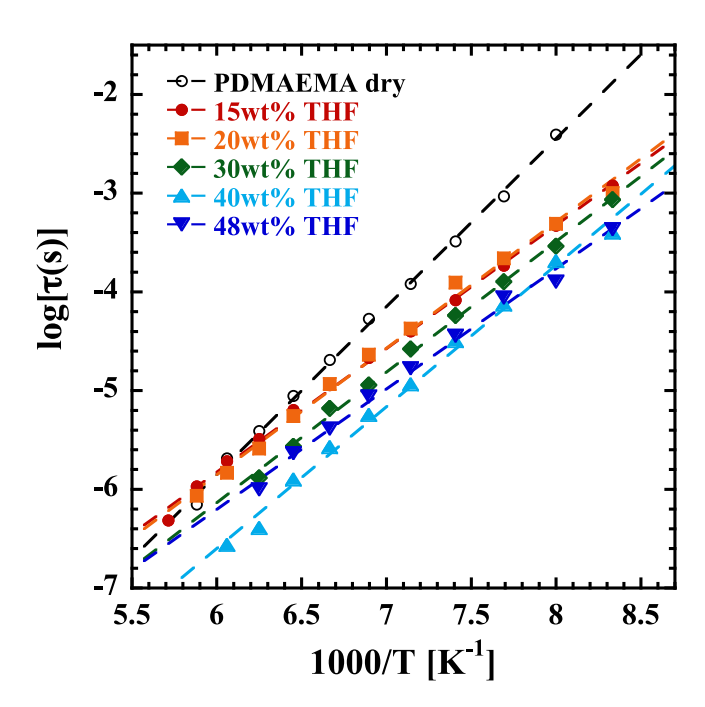


FIG. 11. Inverse temperature dependence of the characteristic times of the PDMAEMA β -relaxation in the dry state (empty symbols) and in THF mixtures (filled symbols). Dashed lines are Arrhenius fits.

Fig. 11]. This was successfully described by Arrhenius laws

$$\tau = \tau_0 \exp\left(\frac{E_a}{k_B T}\right). \tag{6}$$

The obtained parameters are shown in Table III. Within the uncertainties, the relaxation times of all mixtures present a rather similar activation energy, which is clearly lower than that of PDMAEMA in the dry state. In addition, the values of the prefactors τ_0 in the mixtures are reasonable to correspond to an inverse attempt frequency, contrarily to the case of dry PDMAEMA. All these findings point to the presence of two contributions to the β -relaxation of dry PDMAEMA. The faster component would persist upon THF addition, while the slower contribution would be suppressed by the presence of the plasticizer. Thus, the present investigation strongly supports the scenario proposed in the previous DS and QENS work³² and demonstrates that the suppression is dramatic even for very small amounts of added THF molecules.

TABLE III. Arrhenius parameters of the characteristic times of PDMAEMA β -relaxation in THF mixtures at different solvent concentrations. The prefactor of the THF process (with activation energy fixed to E_a = 500 meV) is also listed

	PDMAEMA	THE	
c wt. %	$E_a (\text{meV})$	$\log[\tau_0(s)]$	THF $\log[\tau_0(s)]$
0	340 ± 10	-16.1 ± 0.2	
15	250 ± 15	-13.3 ± 0.4	-18.2 ± 0.1
20	255 ± 15	-13.5 ± 0.4	-18.1 ± 0.1
30	260 ± 15	-14.1 ± 0.4	-18.8 ± 0.1
40	280 ± 15	-15.2 ± 0.4	-20.0 ± 0.1
48	240 ± 20	-13.5 ± 0.4	-19.2 ± 0.1



C. Solvent dynamics

1. H₂O

It has been reported that water dynamics in solutions of hydrophilic polymers, biopolymers, and small glass-forming materials shows a series of universal features.²⁴ Particularly, at temperatures below 200 K there is a water related dielectric relaxation with characteristic times following an Arrhenius temperature dependence with an activation energy close to 540 meV. Moreover, in most of the systems investigated, the temperature dependence of the water relaxation time changes from the Arrhenius-like behavior at low temperatures towards a stronger dependence resembling that of a liquid-like Vogel-Fulcher behavior at higher temperature.^{21,24,26} Interestingly, a similar behavior has also been found for the water dynamics confined in rigid nanostructures.^{27,29} The characteristic times for water dynamics in the mixtures with PDMAEMA are plotted in Fig. 12(a) as function of the inverse

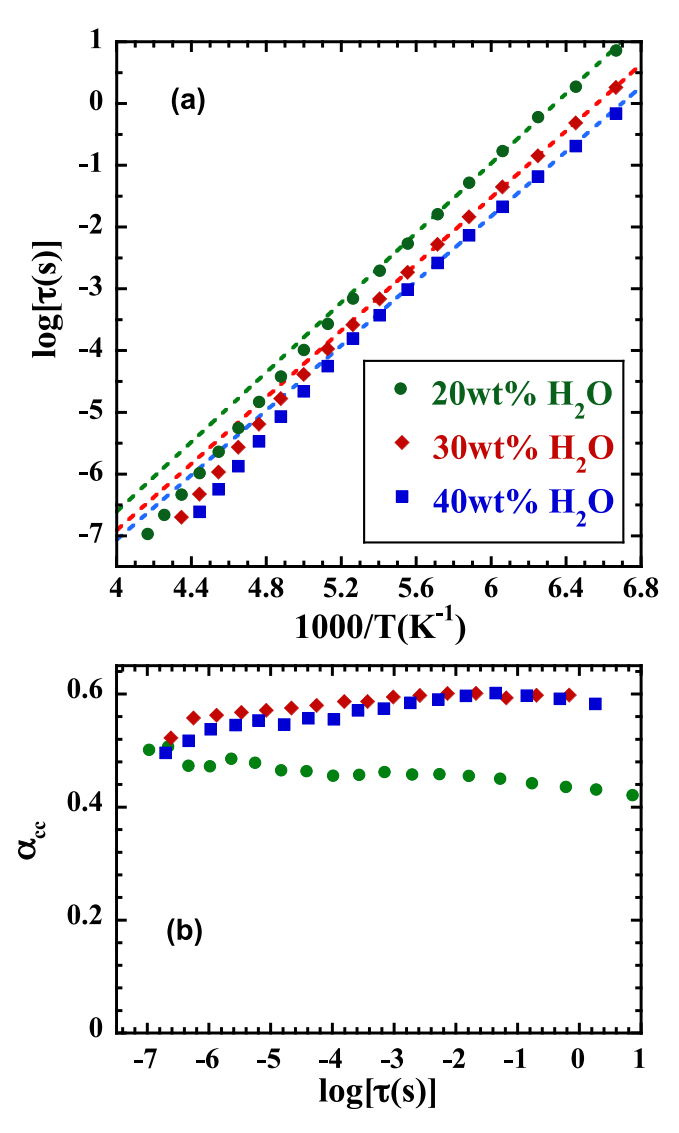


FIG. 12. Parameters characterizing the dynamics of water in aqueous PDMAEMA mixtures at the water concentrations indicated: (a) Inverse temperature dependence of the relaxation times. Dashed lines are Arrhenius fits of the low temperature results. (b) Shape parameter $\alpha_{\rm cc}$ as function of the characteristic time.

temperature. For the three concentrations investigated, they show a similar behavior. At low temperatures the process exhibits an Arrhenius-like dependence. Table IV compiles the values for E_a and $\log(\tau_0)$ obtained from the Arrhenius low-temperature description. We notice a slight reduction of the activation energy as the concentration increases but, within the uncertainties, the values are in the range reported for the "universal" water related dielectric relaxation above described.

Regarding the width of the relaxation function, the values of the α_{cc} -parameter are shown in Fig. 12(b) as function of the characteristic time. Note that the low temperature Arrhenius regime corresponds to characteristic times larger than $\approx 10^{-3}$ s. The α_{cc} -values observed in this region reveal a broader distribution of relaxation times at $c^{H_2O} = 20$ wt. %. This suggests a rather inhomogeneous environment at such low water concentration, while, increasing the water amount, the environment around the water molecule would become more uniform. This is in accord with similar results found in other hydrated polymers. 48

Figure 13 displays the reduced dielectric strength as function of water concentration for both mixtures. This

TABLE IV. Activation energy (E_a) and pre-exponential factor $[\log(\tau_0)]$ of the characteristic times of water in PDMAEMA mixtures at low temperatures as obtained from an Arrhenius fit.

c wt. %	$\log[\tau_0(s)]$	$E_a (\text{meV})$
20	-17.9 ± 0.3	560 ± 10
30	-17.7 ± 0.3	535 ± 10
40	-17.5 ± 0.2	520 ± 10

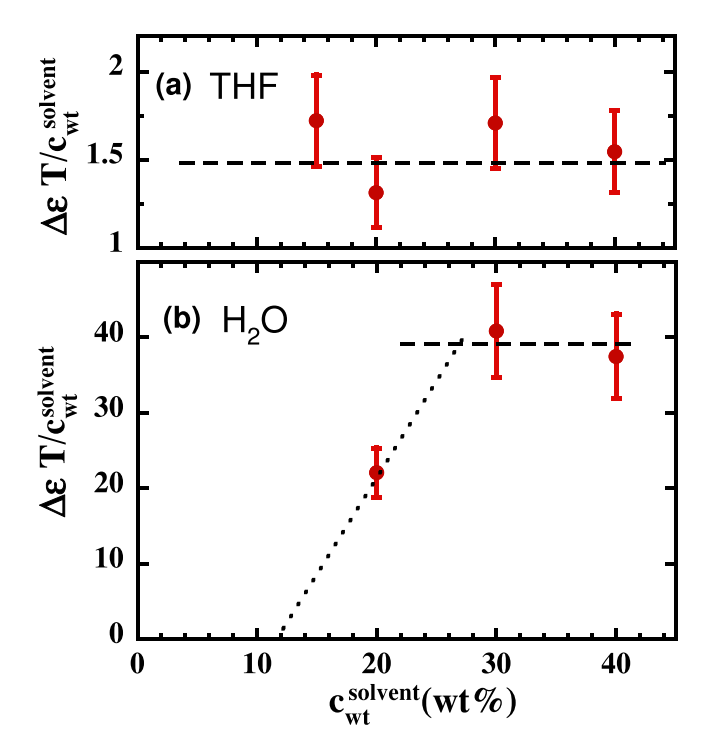


FIG. 13. Solvent-concentration dependence of the reduced dielectric strength of the solvent processes in THF (a) and aqueous mixtures (b). Lines are guides for the eye.



quantity has been defined as $\Delta \epsilon T_R/c^{solvent}$, where $\Delta \epsilon$ corresponds to a temperature T_R at which the loss peak is well centered in the experimental window ($\approx 10^3$ Hz). In this way we remove the trivial effects of temperature and solvent concentration. While for THF we observe a nearly constant behavior, for water this quantity drops dramatically when decreasing the concentration below ≈30 wt. %. A similar behavior has been found in other aqueous solutions.^{21,48} It has been suggested that at low concentration the reorientation of the water dipole moment is somehow restricted, reflecting a strong interaction with the polymer. Increasing the water amount, water molecules would tend to join together leading to the presence of water clusters in the sample. As a consequence, water molecules could orientate more easily, as water-water interactions are more advantageous than those with the PDMAEMA. Hence, the dielectric strength increases more than expected according to the extrapolation from low concentrations. This is in fact the behavior here reported, also in agreement with the finding of evidences for the presence of clusters already at the lowest concentration here investigated.

Above a given temperature, the temperature dependence of the water process becomes more pronounced than the Arrhenius law observed at low temperatures, which, as aforementioned, has also been found in other hydrated systems. In order to establish the possible connection of this crossover temperature T_c with the glass transition of the mixtures, we have calculated the apparent activation energy E_{app} as

$$E_{app} = k_B \frac{d(\ln \tau)}{d(1/T)}. (7)$$

The results are shown in Fig. 14. Within the uncertainties, E_{app} starts increasing with respect to the low-temperature value at around 180 K, independently of concentration. This value of T_c is lower that those usually reported in the literature, most of them lying around 200-220 K. We recall that T_c has usually been identified with the average glass-transition temperature of the system. In our case, T_c coincides with $T_{g,onset}^{DSC}$. The exceptionally broad feature of the glass-transition process in our samples has allowed distinguishing this difference. This finding emphasizes even more the role of the matrix mobility as the main responsible of the crossover of water dynamics behavior in these mixtures.

2. THF

The question now is whether we observe a crossover for THF dynamics in the mixtures. In the previous work on the sample with $c^{THF}=30\,$ wt. %, 33 the dynamical process observed for THF by DS was characterized by an Arrhenius-like temperature dependence of the characteristic time which persists over more than 9 orders of magnitude in time. Thus, no evidences for such a crossover could be identified. The QENS results put forward the restricted nature of this process, determining a size of about 8 Å for the volume within which THF hydrogens' motions are restricted.

Figure 15 shows the characteristic relaxation times of the THF process for the different concentrations investigated.

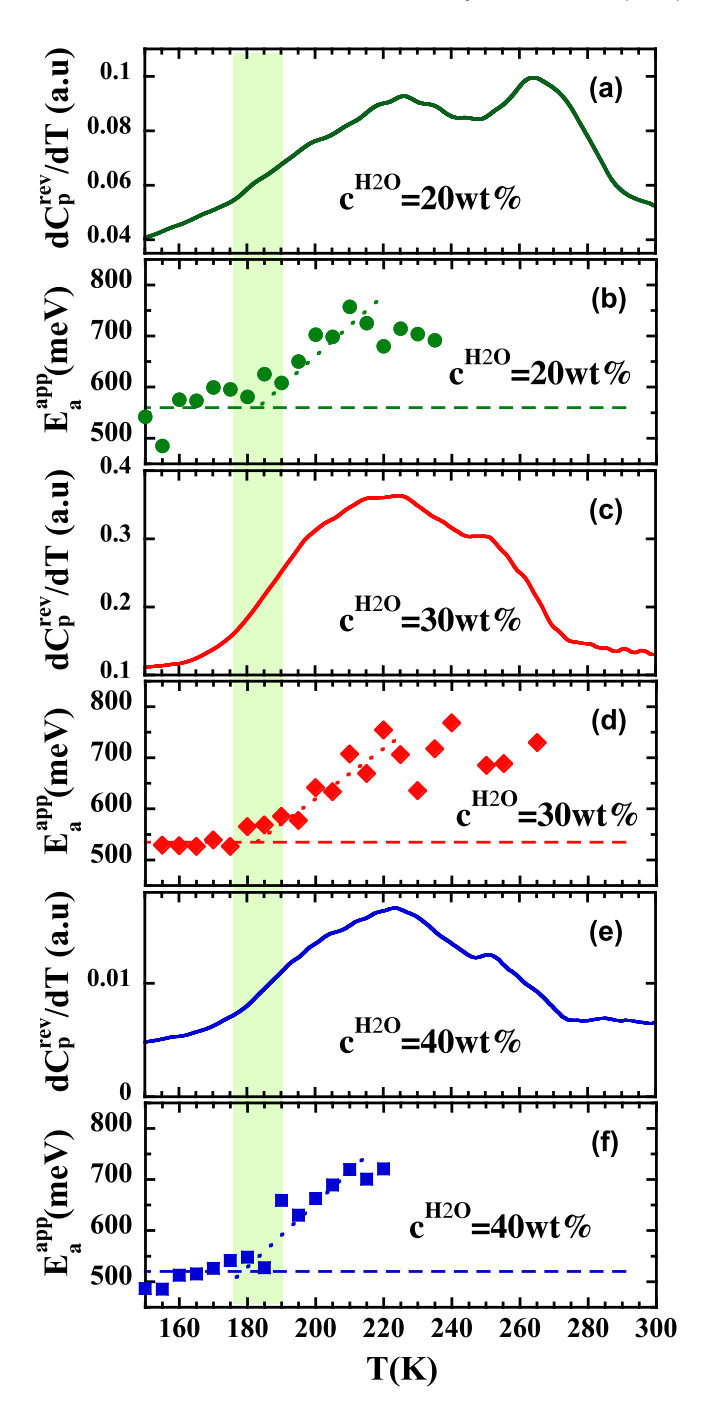


FIG. 14. Temperature dependence of the temperature derivative of the reversible specific heat (a,c,e) and the apparent activation energy of the water process in PDMAEMA/water solutions (b,d,f) for the three concentrations investigated. Horizontal dashed lines show the average activation energy describing the Arrhenius behavior observed at low temperature [see Fig. 12(a), Table IV]; dotted lines are guides to the eye for the higher temperature behavior. The shadowed area indicates the range where both lines meet.

Solvent dynamics becomes faster as its concentration is increased with exception of the 48 wt.% concentration, where the relaxation times become larger than those at 40 wt.%—another signature of the particularity of this high concentration. For all compositions, the results are well described by single Arrhenius laws [Eq. (6)] with the same activation energy ($E_a = 500 \pm 7$ meV) in the whole temperature range investigated. Thus, no signatures of the crossover are revealed.

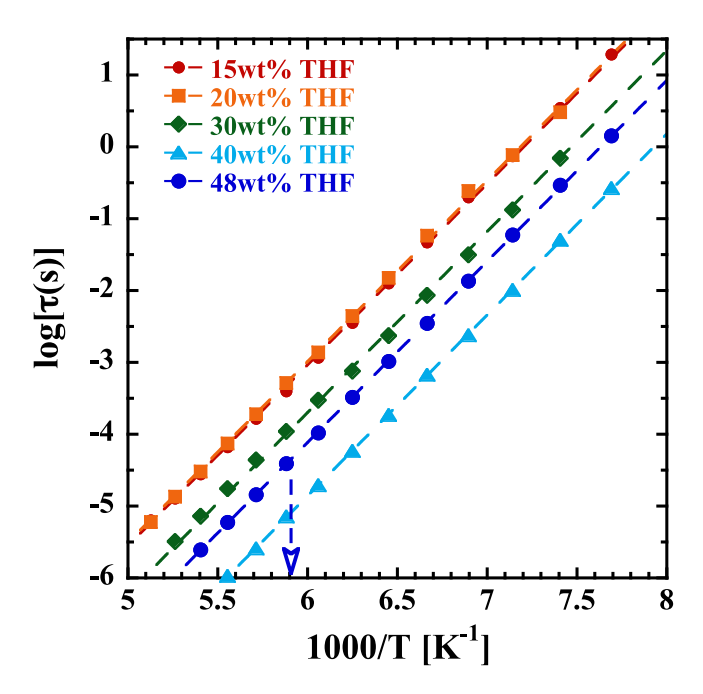


FIG. 15. Inverse temperature dependence of the characteristic times of the relaxation of THF in PDMAEMA/THF mixtures at the THF concentrations indicated. Dashed lines are fits with Arrhenius laws with fixed activation energy $E_a = 500$ meV. Dashed arrow marks the location of T_g^{DSC} corresponding to $c^{THF} = 48\%$.

Regarding the shape of the relaxation, it is possible to identify two different situations. At high THF concentrations (40 and 48 wt.%) the $\alpha_{\rm cc}$ -parameter shows clearly smaller values ($\alpha_{\rm cc}=0.25-0.30$) than for the samples with a lower amount of THF ($\alpha_{\rm cc}=0.29-0.37$), reflecting the structural heterogeneities identified for higher concentrations.

We also comment that we cannot discard that some fraction of the dielectric response attributed to the α -relaxation of PDMAEMA is in fact due to reorientations of THF molecules coupled with the polymer and participating in the main structural relaxation. This situation has been reported in some binary mixtures. 2,49,50

3. THF vs water

In the following we address the question: what could be the reasons for such a different behavior of these solvents?

One favorable ingredient to observe the crossover in the DS window for the aqueous mixtures is the very low value of $T_{g,onset}^{DSC} \approx 180$ K. In the samples with $c^{THF} \gtrsim 40$ wt. % the value of $T_{g,onset}^{DSC}$ is comparable or should be even lower. However, as illustrated in Fig. 15 for the highest concentration, no hints for deviations from the Arrhenius dependence can be noticed, even in the neighborhood of T_g^{DSC} . We could argue that possible crystallization at this concentration may be the reason. As can be appreciated in this figure, the crossover is also missing on the DS data of the $c^{THF} = 40$ wt. % sample, which does not present this kind of problems. Directly comparing the results on both solvents at the same concentration c = 40 wt. % in Fig. 16, we realize that THF dynamics is about three orders of magnitude faster than water dynamics in the mixtures. Therefore, for THF the crossover—

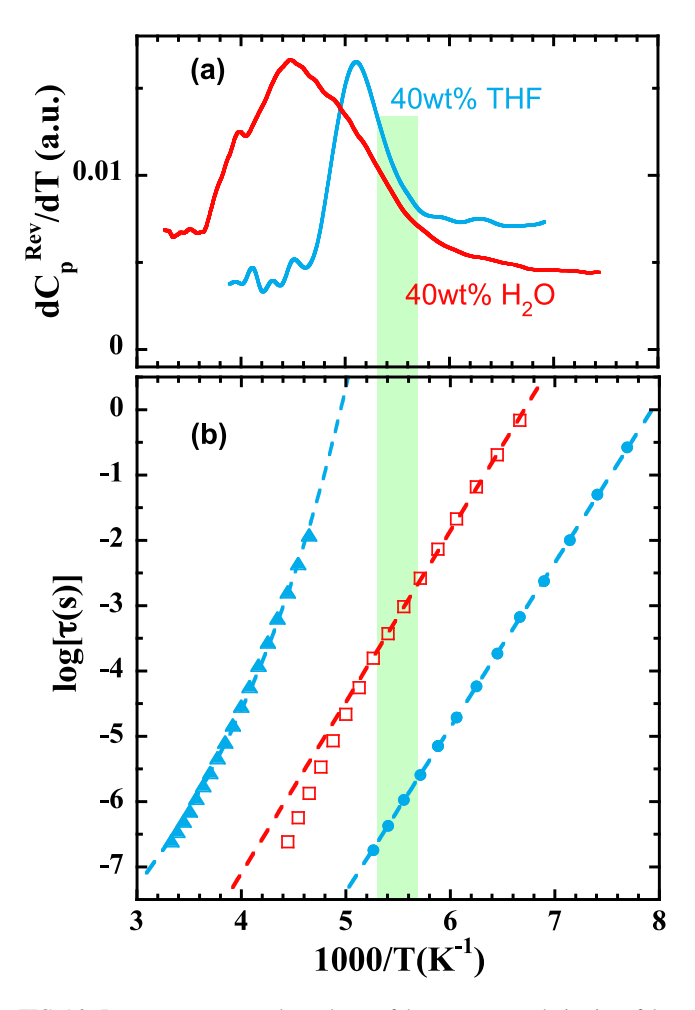


FIG. 16. Inverse temperature dependence of the temperature derivative of the reversible specific heat (a) and the characteristic times of the water component obtained by DS (b) in mixtures with 40 wt. % solvent concentration. Blue color corresponds to the mixture wit THF as solvent and red color to the aqueous solution. In (b), triangles display the α -relaxation and circles the THF relaxation. Squares represent the water process. Dashed lines are VF or Arrhenius fits (see the text). Shadowed area indicates the onset region of the calorimetric glass transitions.

if it exists—should occur in the range of characteristic times of about 10^{-7} s, i.e., demanding methods accessing higher frequencies. We have tried to extend the dielectric study on this sample by a high frequency dielectric spectrometer. Unfortunately, the contribution to the data from the "excess wing" of the α -process has prevented a reliable determination of the characteristic time in such frequency range. We note that, due to its low value, the Arrhenius prefactor for this THF dynamical process cannot be attributed to a realistic attempt frequency. Therefore, at some point there should be a change in the temperature dependence of this process toward a lower activation energy. Such kind of behavior has recently been reported for methyl-THF in polystyrene.⁵¹ To detect this effect, other kind of measurements selective for the THF component dynamics and extending the dynamic range would be required, like, e.g., QENS. With the results at hand, what we can firmly state is the absence of crossover for THF dynamics in the dynamic window explored in this work.

We speculate that in the case of water in polymer matrices, ^{21,24–26} the crossover is observed due to the strong



cooperativity effects on the dynamics of water molecules within the sample. With decreasing temperature, these effects become progressively enhanced, down to the region where the characteristic time of this relaxation reaches high values (of the order of microseconds or even longer). Apparently, THF motions in the mixtures with PDMAEMA do not experience such a pronounced cooperativity. The results on the two kinds of mixtures would be understood assuming that the key ingredient for developing cooperativity effects is the direct interaction between solvent molecules. This is favored if there is a significant number of nearest neighbors of the same nature around a given solvent molecule. This situation is found if the solvent forms clusters, as we have demonstrated for water molecules interacting via H-bonds in our mixtures. On the contrary, specially at concentrations $c^{THF} \leq 30$ wt. %, THF molecules seem to be screened from each other by the side-groups of the polymer. Though at higher concentrations we expect an enhancement of the THF/THF interactions, this seems not to be enough to lead to a significant fraction of cooperatively relaxing THF-regions in the mixtures.

We finally comment on the possibility of the presence of a glass transition associated to the THF component in the mixtures, as it has been reported for mixtures of THF or methyl-THF with other polymers.² If present, this transition would be expected at very low temperatures, in the range of 120-130 K [see Figs. 15 and 16(b)]. To address this question, we have extended the DSC study to lower temperatures on the sample with 30 wt. % (maximum concentration without hint of crystallization). The results can be found in Figure S1 of the supplementary material.⁵² They show no clear hint for a glass-transition process in this range, though its presence cannot either be completely discarded.

VI. CONCLUSIONS

Our structural analysis indicates that THF molecules tend to homogeneously accommodate within the PDMAEMA nano-domains, being predominantly surrounded by polymeric side-groups. However, above a saturation concentration of one THF molecule/monomer, a more heterogeneous situation is found where some of the nano-domains have to expand to put up more THF molecules, which interact also with each other. Nevertheless, clear evidences for clusters, like a well defined peak in the diffraction pattern, are not found in THF mixtures. On the contrary, water molecules—much smaller than THF molecules and strongly interacting via H-bonding have a pronounced tendency to cluster. Aqueous mixtures are characterized by a highly heterogeneous structure where water clusters coexist with an underlying nano-segregation of main chains and side groups of the polymeric matrix. We have identified a change in the intra-cluster structural features that could be attributed to a variation of water/water and water/polymer interactions in the range 230 K $\leq T \leq$ 260 K. In addition, rearrangements of the structure at nano-domain and inter-cluster level occur at high temperatures, where all the polymeric chains can move, the most hydrated as well as the driest regions.

The dynamics (α and β -processes) of the polymer component in the mixtures with THF-accessed by both, DSC and DS techniques—are strongly affected by the solvent. We observe a remarkable reduction of the glass-transition temperature and a "stronger" behavior of the α -relaxation of PDMAEMA even at the lowest THF concentration investigated (15 wt. %). The plasticization effect is enhanced with increasing amount of THF but seems to reach saturation at c_w^{THF} = 40 wt. %—where presumably some THF molecules start to interact with each other. Regarding the β -relaxation, a rather similar activation energy is found in all the mixtures, which is markedly lower than that found in the dry sample. This could indicate that, already at $c_w^{THF} = 15$ wt. %, a slow component of PDMAEMA β -relaxation observed in the dry state is highly hindered by the presence of solvent molecules, as it was proposed in our previous work.³²

The source for information about polymer dynamics in aqueous solutions is DSC. These results evidence a strikingly broad glass-transition feature, revealing a highly heterogeneous behavior in agreement with the conclusions from the structural study. Independent of the macroscopic composition, there seems to be a preferential local concentration in the aqueous mixtures, the glass-transition associated to which is similar to that found in the THF mixtures with $c_w^{THF}=30$ wt. % (i.e., where all monomers are affected by the solvent molecules). The DSC results for the 20 wt. % water content, i.e., about 2.7 water molecules/monomer, reveal a bimodal feature that could be attributed to the presence of much poorly hydrated regions than the average—a kind of phase-separated situation.

Deep in the glassy state—below the onset of the glass transition—the dynamics of both solvents can be described by an Arrhenius temperature dependence with a rather similar activation energy. However, the values of the characteristic times are about three orders of magnitude smaller for THF than for water. Increasing the temperature, a crossover is found toward increasingly higher apparent activation energies for water molecules, while the same Arrhenius law persists in the case of THF. We note that we have identified the crossover temperature in the aqueous samples with the onset of the glass transition and not with the average glass transition. This assignment becomes clear in these samples because the glass-transition process is particularly broad—a property probably induced by the nano-domain underlying structure of the polymer matrix—and strongly supports the interpretation of the crossover as a consequence of the freezing of the structural relaxation of the surrounding matrix. The absence of a crossover (at least in the wide dynamic window here accessed) for THF is attributed to the lack of cooperativity effects in the relaxation of these molecules. We hypothesize that these effects only arise if the number of nearest neighbors of the same nature around a given solvent molecule is above a certain threshold. That is, they can appear in clusters like those formed by water molecules but are not developed for THF molecules in the mixtures—THF molecules are screened from each other by the polymeric side groups for $c_w^{THF} \le 30$ wt. %, and start to experience direct interactions with other THF molecules at higher concentrations. However, crystallization enters the



game in the THF mixtures before clusters formation can be resolved.

ACKNOWLEDGMENTS

We thank Dr. A. Iturrospe for her help with the XR-diffraction measurements and Dr. Remi Busselez for helpful discussions. Financial support from the Projects Nos. MAT2012-31088 and MAT2015-63704-P (Spanish-MINECO and EU) and IT-654-13 (Basque Government) is acknowledged. This work is based on experiments performed at SANS-2 (SINQ, Paul Scherrer Institute, Villigen, Switzerland), and DNS-instrument JNSE (Heinz Maier-Leibnitz Zentrum (MLZ), Garching, Germany) and has been supported by the European Commission under the 7th Framework Programme through the "Research Infrastructures" action of the "Capacities" Programme, NMI3-II Grant No. 283883.

- ¹H. Takeno, S. Koizumi, H. Hasegawa, and T. Hashimoto, Macromolecules **29**, 2440 (1996).
- ²T. Blochowicz, S. Lusceac, P. Gutfreund, S. Schramm, and B. Stuhn, J. Phys. Chem. B 115, 1623 (2011).
- ³G. A. Schwartz, J. Colmenero, and Á. Alegría, Macromolecules 40, 3246 (2007).
- ⁴R. Pérez Aparicio, A. Arbe, J. Colmenero, B. Frick, L. Willner, D. Richter, and L. Fetters, Macromolecules **39**, 1060 (2006).
- ⁵M. Brodeck, F. Alvarez, J. Colmenero, and D. Richter, Macromolecules 45, 536 (2011).
- ⁶S. Arrese-Igor, A. Alegría, A. Moreno, and J. Colmenero, Macromolecules 44, 3611 (2011).
- ⁷J. Colmenero and A. Arbe, Soft Matter 3, 1474 (2007).
- ⁸A.-C. Genix, A. Arbe, F. Alvarez, J. Colmenero, L. Willner, and D. Richter, Phys. Rev. E 72, 031808 (2005).
- ⁹A. Arbe, A. Alegria, J. Colmenero, S. Hoffmann, L. Willner, and D. Richter, Macromolecules 32, 7572 (1999).
- ¹⁰I. Cendoya, A. Alegria, J. Alberdi, J. Colmenero, H. Grimm, D. Richter, and B. Frick, Macromolecules 32, 4065 (1999).
- ¹¹J. W. Sy and J. Mijovic, Macromolecules 33, 933 (2000).
- ¹²S. Zhang and J. Runt, J. Polym. Sci., Part B: Polym. Phys. **42**, 3405 (2004).
- ¹³D. A. Savin, A. M. Larson, and T. P. Lodge, J. Polym. Sci., Part B: Polym. Phys. **42**, 1155 (2004).
- ¹⁴T. Hashimoto, J. Polym. Sci., Part B: Polym. Phys. **42**, 3027 (2004).
- ¹⁵D. Bingemann, N. Wirth, J. Gmeiner, and E. A. Rossler, Macromolecules 40, 5379 (2007).
- ¹⁶ A. K. Rizos, R. M. Johnsen, W. Brown, and K. L. Ngai, Macromolecules 28, 5450 (1996).
- ¹⁷M. Tyagi, A. Arbe, A. Alegría, J. Colmenero, and B. Frick, Macromolecules
- ¹⁸D. Schwahn, V. Pipich, and D. Richter, Macromolecules **45**, 2035 (2012).
- ¹⁹S. Sudo, S. Tsubotani, M. Shimomura, N. Shinyashiki, and S. Yagihara, J. Chem. Phys. **121**, 7332 (2004).

- ²⁰S. Cerveny, G. Schwartz, A. Alegria, R. Bergman, and J. Swenson, J. Chem. Phys. **124**, 194501 (2006).
- ²¹S. Cerveny, A. Alegría, and J. Colmenero, J. Chem. Phys. **128**, 044901 (2008).
- ²²T.-X. Xiang and B. D. Anderson, Pharm. Res. **22**, 1205 (2005).
- ²³M. Laurati, P. Sotta, D. Long, L.-A. Fillot, A. Arbe, A. Alegria, J. Embs, T. Unruh, G. Schneider, and J. Colmenero, Macromolecules 45, 1676 (2012).
- ²⁴S. Cerveny, Á. Alegría, and J. Colmenero, Phys. Rev. E **77**, 031803 (2008).
- ²⁵R. Busselez, A. Arbe, S. Cerveny, S. Capponi, J. Colmenero, and B. Frick, J. Chem. Phys. **137**, 084902 (2012).
- ²⁶J. Swenson and S. Cerveny, J. Phys.: Condens. Matter 27, 033102 (2015).
- ²⁷S.-H. Chen, L. Liu, E. Fratini, P. Baglioni, A. Faraone, and E. Mamontov, Proc. Natl. Acad. Sci. U. S. A. **103**, 9012 (2006).
- ²⁸A. Faraone, L. Liu, C.-Y. Mou, C.-W. Yen, and S.-H. Chen, J. Chem. Phys. 121, 10843 (2004).
- ²⁹M.-C. Bellissent-Funel, K. Kaneko, T. Ohba, M.-S. Appavou, A. J. Soininen, and J. Wuttke, Phys. Rev. E 93, 022104 (2016).
- ³⁰H. Wang, L. Wang, P. Zhang, L. Yuan, Q. Yu, and H. Chen, Colloids Surf., B 83, 355 (2011).
- ³¹E. Wagner and J. Kloeckner, Polym. Ther. I **192**, 135 (2006).
- ³²G. Goracci, A. Arbe, A. Alegría, V. García Sakai, S. Rudic, G. J. Schneider, W. Lohstroh, F. Juranyi, and J. Colmenero, Macromolecules 48, 6724 (2015).
- ³³G. Goracci, A. Arbe, A. Alegría, W. Lohstroh, Y. Su, and J. Colmenero, J. Chem. Phys. **143**, 094505 (2015).
- ³⁴A. J. Moreno, A. Arbe, and J. Colmenero, Macromolecules **44**, 1695 (2011).
- ³⁵A. Arbe, A.-C. Genix, J. Colmenero, D. Richter, and P. Fouquet, Soft Matter 4, 1792 (2008).
- ³⁶M. Beiner and H. Huth, Nat. Mater. **2**, 595 (2003).
- ³⁷A.-C. Genix and F. Lauprêtre, Macromolecules 38, 2786 (2005).
- ³⁸C. Gerstl, M. Brodeck, G. Schneider, Y. Su, J. Allgaier, A. Arbe, J. Colmenero, and D. Richter, Macromolecules 45, 7293 (2012).
- Iradi, F. Alvarez, J. Colmenero, and A. Arbe, Phys. B 350, E881 (2004).
 Busselez, A. Arbe, F. Alvarez, J. Colmenero, and B. Frick, J. Chem. Phys.
- ⁴⁰R. Busselez, A. Arbe, F. Alvarez, J. Colmenero, and B. Frick, J. Chem. Phys **134**, 054904 (2011).
- ⁴²M. Wind, R. Graf, S. Renker, H. W. Spiess, and W. Steffen, J. Chem. Phys. 122, 014906 (2005).
- ⁴³S. Hiller, O. Pascui, H. Budde, O. Kabisch, D. Reichert, and M. Beiner, New J. Phys. 6, 10 (2004).
- ⁴⁴N. Floquet, J. P. Coulomb, N. Dufau, G. Andre, and R. Kahn, Adsorption 11, 139 (2005).
- ⁴⁵R. Mancinelli, J. Phys.: Condens. Matter **22**, 404213 (2010).
- ⁴⁶Broadband Dielectric Spectroscopy, 2003rd ed., edited by F. Kremer and A. Schönhals (Springer, 2002).
- ⁴⁷M. Wübbenhorst and J. van Turnhout, Dielectr. Newsl. 14, 1 (2000), available at http://www.novocontrol.de/newsletter/DNL14.PDF.
- ⁴⁸S. Cerveny, J. Colmenero, and A. Alegria, Macromolecules **38**, 7056 (2005).
- ⁴⁹D. Bock, R. Kahlau, B. Pötzschner, T. Körber, E. Wagner, and E. Rössler, J. Chem. Phys. **140**, 094505 (2014).
- ⁵⁰R. Kahlau, D. Bock, B. Schmidtke, and E. Rössler, J. Chem. Phys. **140**, 044509 (2014).
- ⁵¹T. Blochowicz, S. Schramm, S. Lusceac, M. Vogel, B. Stühn, P. Gutfreund, and B. Frick, Phys. Rev. Lett. **109**, 035702 (2012).
- $^{52} See$ supplementary material at http://dx.doi.org/10.1063/1.4946004 for DSC results on the sample with 30 wt.% of THF extended down to 100 K.

